



Constraints on the current rate of deformation and surface uplift of the Australian continent from a new seismic database and low-T thermochronological data

J. BRAUN¹*, D. R. BURBIDGE², F. N. GESTO³, M. SANDIFORD⁴, A. J. W. GLEADOW⁴, B. P. KOHN⁴ AND P. R. CUMMINS²

¹Géosciences Rennes, Université de Rennes 1, CNRS, Rennes, 35042 Cedex France.

²Geoscience Australia, GPO Box 378, Canberra, ACT 2601, Australia.

³Research School of Earth Sciences, Australian National University, ACT 0200, Australia.

⁴School of Earth Sciences, University of Melbourne, Vic. 3052, Australia.

Estimates of the current rate of deformation and surface uplift for the Australian continent are derived by integration of a new seismic database and show that parts of the continent are currently experiencing deformation at a rate of $1\text{--}5 \times 10^{-16}/\text{s}$ and uplifting at a rate of 10–50 m/Ma. In the east, these regions coincide with the regions of maximum topography, suggesting that, if this uplift rate is long-term, up to 50% of the present-day topographic relief in the southeastern Highlands and Flinders Ranges has formed in the last 10 Ma, i.e. the time we estimate for the onset of the present-day stress field experienced by the Indo-Australian Plate. These estimates are supported by fission-track data from the Snowy Mountains, which indicate that a non-negligible proportion of the present-day relief is the remnant of a much older topography formed during the various accretion or breakup events along the eastern margin of the continent in Late Paleozoic to Early Mesozoic time and that younger relief growth (i.e. younger than 100 Ma) must be limited to less than a kilometer in amplitude. By contrast, in the western part of the continent no such correlation exists between present-day topography and uplift predicted by integrating seismic strain rate over 10 Ma. This suggests that the apparently high level of seismic activity observed in the southwestern part of the Yilgarn Craton and along Proterozoic mobile belts, such as the Albany–Fraser Province of southeastern Western Australia and the Fitzroy Trough of northern Western Australia, is transient or that, contrary to what is happening in the east, erosional processes are able to remove surface relief created at the relatively slow rate of 10 m/Ma, potentially because there existed no finite amplitude topography prior to the onset of the present-day compressional stress field.

KEY WORDS: Australia, neotectonics, seismicity, strain rate, topography.

INTRODUCTION

It has been recently proposed that parts of the Australian continent are not as tectonically quiet as previously thought (Sandiford 2003a). Evidence includes Quaternary fault movement in the Neoproterozoic Adelaide Fold Belt and in the Paleozoic Lachlan Fold Belt (Kohn *et al.* 1999; Sandiford 2003a), prominent range-bounding scarps (Sandiford 2003a), a Late Miocene regional unconformity in neighbouring basins (Dickinson *et al.* 2002) and diffuse seismicity (Denham 1988). In the east, these regions are also characterised by a relatively high surface topography (i.e. compared with the rest of the continent) and are also the locus of most of the present-day seismicity (Doyle 1971; Denham 1988), suggesting that some of the topography may be the result of ongoing deformation, rather than the remnant of old Paleozoic or

Early Mesozoic mountain belts. This deformation is thought to be caused by a continental-scale state of compression originating from orogenic events along three of the Indo-Australian Plate boundaries: the Himalayan collision, the Papua New Guinea fold-and-thrust belt and the Southern Alps of New Zealand (Coblentz *et al.* 1995; Reynolds *et al.* 2002; Sandiford *et al.* 2004). If this is the case, the current state of stress would be approximately 5–10 Ma (i.e. the time at which the collision across the South Island of New Zealand initiated: Batt & Braun 1999; Batt *et al.* 2000).

Seismicity is evidence for brittle deformation of the upper crust. The magnitude distribution and frequency of earthquakes is intuitively related to the rate of brittle deformation. Here we use a newly compiled seismic database for the Australian continent to compute a lower bound estimate of the present-day distribution of

*Corresponding author: jean.braun@univ-rennes1.fr

brittle strain rate and, by extrapolation, the total amount of strain and uplift experienced in the last 10 Ma. We compare these estimates with the present-day topography to help constrain how much of the topography is related to recent surface uplift (i.e. younger than 10 Ma). The method relies on a statistically significant knowledge of the current seismicity and on the observation that most earthquakes in Australia are compressive, and therefore the brittle deformation they represent contributes to horizontal contraction and uplift.

STATE OF STRESS

Australia is often regarded as the oldest continent on Earth. This reflects our perception that it is partly made of relatively old crustal blocks (such as the Archean Yilgarn and Pilbara Cratons in the west of the continent) but also that its interior has remained tectonically inactive for the last 200 Ma, i.e. approximately since the end of the last accretion event along the eastern margin of the continent in the mid-Triassic (Veevers *et al.* 1984; de Caritat & Braun 1992). During the breakup of Gondwana in the Cretaceous, the continent rifted away from India, Antarctica, Lord Howe Rise and New Zealand (Veevers *et al.* 1984). However, during these times stretching and thinning of the lithosphere were largely confined to the margins of the continent and had little effect on its interior. More recently, i.e. from the Late Eocene to present, the Indo-Australian Plate has experienced a series of compressional events along several of its margins. First collision along the

Indo-Asian collisional front in the Himalayas, started at approximately 50 Ma (Molnar & Tapponnier 1975). Then, in the last 25 Ma, several volcanic arcs accreted along the plate northern margin leading to the development of the New Guinea fold-and-thrust belt (Smith 1990). Most recently in the last 5–10 Ma, rapid oblique convergence has been taking place across the Alpine Fault in the South Island of New Zealand (Wellman 1979; Batt & Braun 1999).

The present-day state of stress in the Australian continent has been extensively studied (Cloetingh & Wortel 1986; Coblenz *et al.* 1995, 1998; Hillis & Reynolds 2000; Reynolds *et al.* 2002; Burbidge 2004). The combined analyses of stress magnitude and orientation and earthquake focal mechanisms show a relatively simple picture (Figure 1). The majority of earthquakes recorded in the Australian continental interior are compressional in nature (Denham 1988), which supports the concept that the continent is under a state of compressive stress, squeezed between the three collisions zones located along the margins of the Indo-Australian Plate. Borehole stress measurements confirm this situation (Hillis & Reynolds 2000). Furthermore, to first order, stress trajectories can be easily reproduced by assuming that the Indo-Australian Plate is 'pinned' along three of its boundaries that experience compressional forces (Figure 1) (Reynolds *et al.* 2002). These forces are transmitted towards the continent interior by the elastic rigidity of the plate leading to a relatively uniform stress field. Most importantly, Sandiford *et al.* (2004) have argue that the neotectonic record of deformation in southeast Australia associated with southeast–northwest-trending axes of maximum horizontal stress

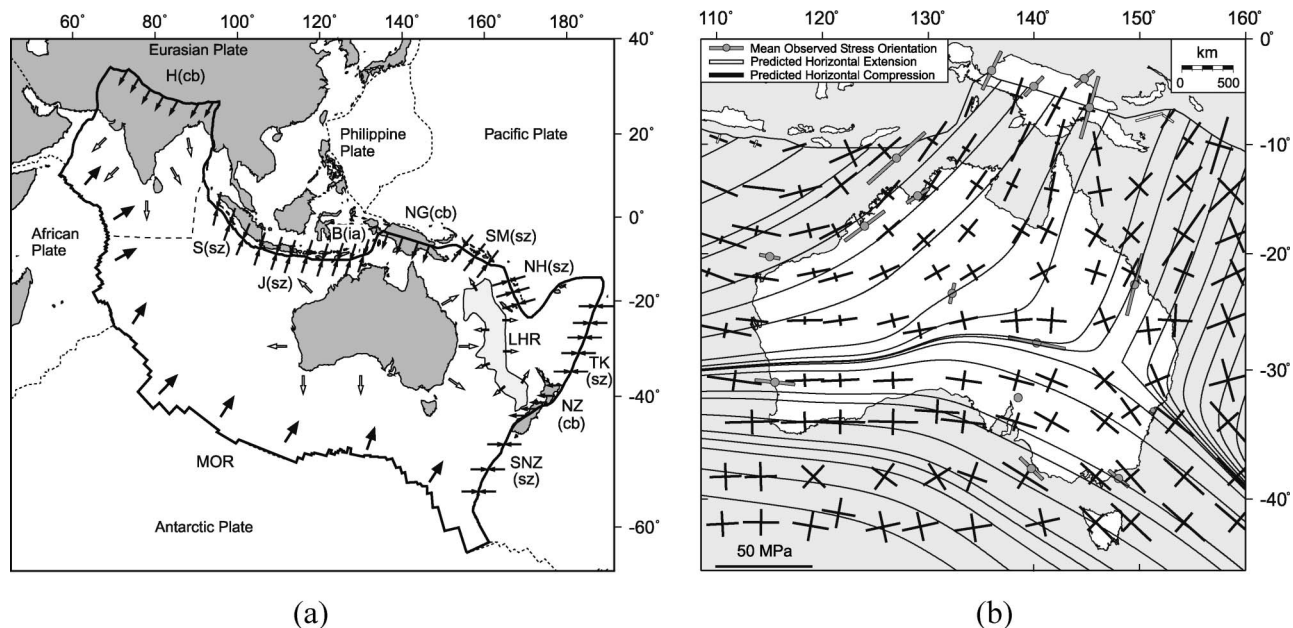


Figure 1 (a) Forces acting along the Indo-Australian Plate. H, Himalaya; S, Sumatra Trench; J, Java Trench; B, Banda Arc; NG, New Guinea; SM, Solomon Trench; NH, New Hebrides; TK, Tonga–Kermadec Trench; NZ, New Zealand; SNZ, south of New Zealand; MOR, mid-ocean ridge; LHR, Lord Howe Rise; cb, collisional boundary; sz, subduction zone; ia, island arc. (b) Stress field within the Australian continent. Stress trajectories as predicted by a thin elastic-plate model driven by forces originating along the plate compressional boundaries, superimposed on averaged stress orientation estimates from large earthquakes and borehole data (from Reynolds *et al.* 2002).

(S_{Hmax}) dates back to between 10 and 5 Ma, coinciding with the initiation of the Southern Alpine 'collision' in New Zealand.

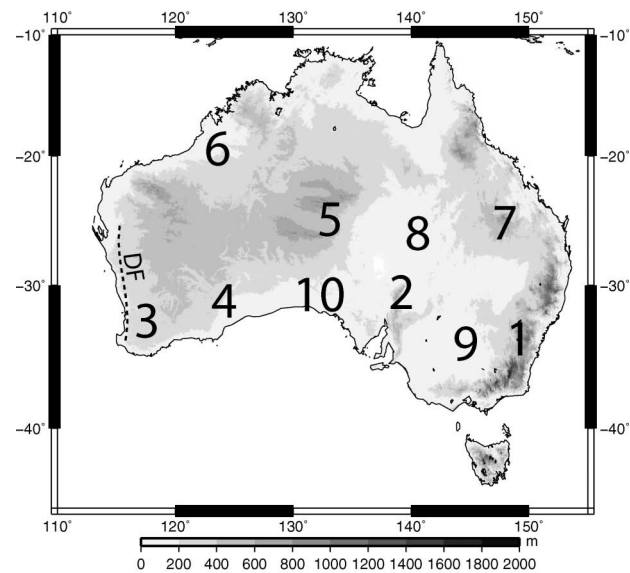
DISTRIBUTION OF SEISMICITY

That the present-day stress field leads to seismic activity in various parts of the continent (Denham 1988) implies that the stress level is sufficiently high to produce brittle deformation of the continental interior. This, in turn, implies that the Australian Plate is locally weak enough for the relatively uniform stress regime originating along its boundaries to cause deformation. The question of why some parts of the continent are deforming and others are not, is linked to our understanding of the rheology of the continental lithosphere which, to date, is incomplete (Maggi *et al.* 2000; Jackson 2002; Watts & Burov 2003).

It is clear that the distribution of seismicity within the Australian continent is not uniform (Figure 2b). Some of the continent passive margins have experienced large earthquakes, such as the Newcastle earthquake ($M_L = 5.5$) in 1989 along the east coast of Australia or the Collier Bay earthquake ($M_w = 6.3$) in 1997 which occurred offshore the northwest coast of Australia. Large events have also been recorded in regions that have been seemingly tectonically inactive for more than half a billion years, such as in the Tennant Creek (Northern Territory) or the Meckering (Western Australia) areas. Other parts of the continent currently experience frequent but low-magnitude earthquakes, such as beneath the southeastern Highlands and the Flinders and Mt Lofty Ranges of South Australia. Recent paleoseismic studies show evidence for relative large magnitude events $M_w > 6.5$ in the Flinders Ranges (Quigley *et al.* 2006). Previous authors have associated this seismicity with the post-tectonic, erosion-driven isostatic rebound of these high-elevation regions (Lambeck *et al.* 1989). However, most of the earthquakes are compressional, which does not support the deformation pattern that one would expect from an isostatically rebounding region. Alternatively, the relationship between seismicity and elevated topography may indicate that the continent is currently deforming and that at least parts of the current topography have been created in the recent past by surface uplift caused by lithospheric shortening. This notion has recently been suggested by Sandiford (2003a, b) for the southeastern part of the continent in the Flinders Ranges in South Australia and the Otway Ranges in Victoria.

In order to estimate the current rate of lithospheric deformation caused by the present-day stress field and the proportion of the current topography that has been created in the recent past (i.e. in the last 10 Ma), we make use of our knowledge of the distribution and magnitude of earthquakes in the Australian continent. To achieve this, we use a newly compiled seismic database. The database was compiled by combining hypocentre lists from a number of agencies including Geoscience Australia, the Department of Primary Industries South Australia, the Seismological Research Centre (part of Environment Systems and Services),

a) Present-day topography



b) Seismicity

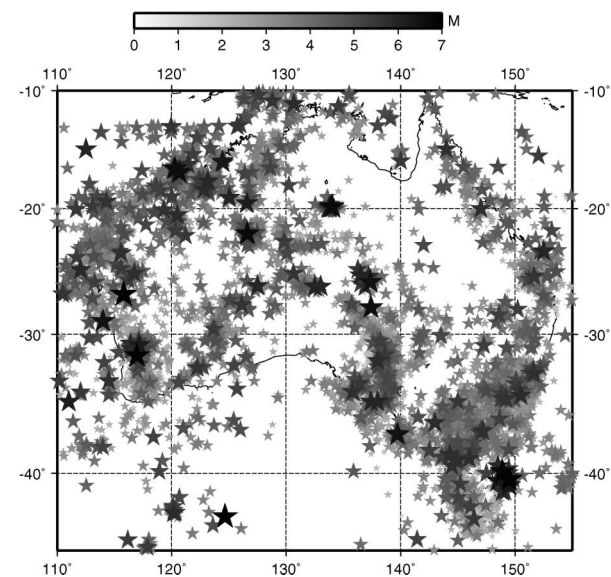


Figure 2 (a) Present-day topography averaged over $1^\circ \times 1^\circ$ cells. 1, southeastern Highlands; 2, Mt Lofty/Flinders Ranges; 3, southwestern Yilgarn Craton; 4, Albany–Fraser Province; 5, central Australian basins; 6, Canning Basin; 7, southeastern Queensland Highlands; 8, Eromanga Basin; 9, Murray Basin; 10, Gawler Craton; DF, Darling Fault. (b) Distribution of seismicity within the Australian continent as observed in the period 1950–2007.

Queensland University, the South East Queensland Water Corporation Ltd, the Research School of Earth Sciences at the Australian National University and the International Seismological Centre. The number of duplicate events in the list is kept to a minimum by not including events in the combined list which are close to any other event in space, time and magnitude. The combined list is the most comprehensive list of

Australian earthquakes yet compiled. In order to determine the seismic strain rate, we need to know the magnitude of each event. Unfortunately, a variety of magnitude scales have been used by each agency and at different times by the same agency. The magnitude scale used here (hereafter referred to as the 'preferred' magnitude, M) was determined according by the following criteria:

Use M_w if available else
 Use M_s if $M_s > 5.5$ else
 Use M_L if available else
 Use M_D if available else
 Use m_b if available else
 Use M_{UNSP} if available else
 Use M_s

where M_{UNSP} denotes an unknown or unspecified magnitude, M_w is moment magnitude, M_s is surface wave magnitude, M_L is local magnitude, M_D is duration magnitude, and m_b is body wave magnitude. Note that some magnitude scales can use different formulae to calculate their final values (e.g. M_L), so using one magnitude scale for all the events and discarding the others is not necessarily going to produce a uniform measure of earthquake size. By including all events with an estimated magnitude, we hope to produce the best possible estimate of the size of the earthquakes, while only discarding the smallest number of events. This list was then further reduced by removing probable aftershocks using the method of Sinadinovski (2000). Only earthquakes after 1970 and with a preferred magnitude > 2 were used in the following calculations. The catalogue is similar to the one used by Leonard (2008) except that it contains an additional one and a quarter year's worth of data [this catalogue contains earthquakes up to April 2007; the catalogue used by Leonard (2008) stopped in 2005].

SEISMIC ACTIVITY AND DEFORMATION

Shallow continental seismicity is evidence for deformation of the brittle upper crust. We can use the distribution and magnitude of the seismicity in the Australian continent observed during the last 50 years to compute an estimate of the brittle strain rate. To achieve this, we use a theoretical relationship between the components of the mean, or integrated, seismic strain rate tensor, $\dot{\epsilon}_{ij}$, and the sum of the seismic moment tensors of each observed earthquake, M_{Oij}^k (Kostrov 1974):

$$\dot{\epsilon}_{ij} = \frac{1}{2\mu\Delta V\Delta t} \sum_{k=1}^N M_{Oij}^k \quad (1)$$

where μ is elastic shear modulus, ΔV is the volume of the crust in which the N earthquakes were observed over a period of time Δt . Under the assumption that the plate boundary forces are the main contributor to the internal plate stress field and, consequently, that this stress field is locally uniform and compressive, we can transform this tensorial relationship into a scalar one, introducing

the mean maximum horizontal shortening strain rate, $\dot{\epsilon}_H$, and the magnitude of the seismic moment, M_0 :

$$\dot{\epsilon}_H = \frac{1}{2\mu\Delta V\Delta t} \sum_{k=1}^N M_0^k \quad (2)$$

Seismic moment is difficult to estimate directly from seismic observations, as it requires a relatively good spatial coverage of seismic stations (i.e. seismic energy/moment release is not isotropic). Here, we have used an empirical relationship relating the amplitude of seismic moment, M_0 , to the magnitude of the earthquake:

$$M_0 = 10^{1.5M+9.1} \quad (3)$$

where M_0 is expressed in Nm (Purcaru & Berckhemer 1978). We will make the assumption that it is of general applicability and that it is appropriate for our 'preferred' magnitude scale. This relationship is appropriate for earthquake magnitude below values where the scale saturates. This occurs around magnitude 7.5 for surface wave magnitudes and lower for body wave magnitudes (Scholz 2004). There are only a handful of earthquakes above 6 in the catalogue, and they generally do not use body wave magnitudes as their 'preferred' magnitude (note that m_b is at the bottom of our list of defined magnitudes to use for any earthquake). Equation 3 is thus appropriate for the entire catalogue. To be accurate the summation must be performed over a time period that is similar to, or larger than, the recurrence time of most earthquakes. For cratonic areas like the Australian continent, the recurrence time of large earthquakes ($M > 6$) is known to be much larger than the observation time (50 years). To improve on the statistical significance of the brittle strain rate estimate, we make use of the Gutenberg–Richter relationship (Gutenberg & Richter 1944), relating the magnitude of earthquakes to their frequency distribution:

$$\log_{10} N = a - bM \quad (4)$$

where N is the number of earthquakes with magnitude M or greater. The value of the parameters a and b varies spatially and can be locally determined from the observed magnitude frequency distribution. Combining equations 2–4 leads to the following expression for the seismic/brittle strain rate:

$$\dot{\epsilon}_H = \frac{1}{2\mu\Delta V\Delta t} \frac{b10^{a+9.1}}{1.5-b} (10^{(1.5-b)M_{\text{max}}}) \quad (5)$$

as a function of the parameters a and b and the maximum magnitude, M_{max} . This expression was derived in Johnston (1994) and also been used to calculate the bulk seismic strain rate of Australia by Triep & Sykes (1997).

The value of the parameters a and b is estimated by least-squares fit (linear regression) of cumulative magnitude frequency relationships constructed from subsamples of the seismic database in $2^\circ \times 2^\circ$ cells. We only considered cells in which there is a minimum of 20

earthquakes. The maximum magnitude bin used in the least-squares fit always had at least one earthquake in it. Cells with a correlation coefficient, r^2 , below 0.95 value (mostly due to catalogue incompleteness) were thrown out. In order to check the results we also tested the effect of removing the first and last magnitude bin on the a and b values and the effect of forcing b to be exactly 1.0, but neither caused the seismic strain rate to change significantly.

The maximum magnitude used in equation 5 was taken to be 7, i.e. somewhere between the magnitude of the largest historical earthquake instrumentally observed in Australia, $M_{\max}=6.7$ or an average for stable continental regions of $M_{\max}=7.5$ (Johnston 1994). ΔV is estimated by multiplying the surface area of the cell by the thickness of the seismogenic layer, h_s . We computed the mean earthquake depth, \bar{h}_s , by averaging the depth estimates provided in the earthquake database in each cell but eventually decided to use an arbitrary value of 15 km for h_s as most depth estimates are relatively uncertain. The resulting predicted distribution of seismic strain rate is shown in Figure 3.

Because the forces that drive deformation of the Australian continent are distant from its interior, i.e. they originate along the plate boundaries, one can assume that there is no net vertical shear of lithospheric columns, and thus that deformation of the brittle upper crust must be accompanied by deformation of the underlying lower crust and lithospheric mantle. One can therefore describe the present-day deformation of the continent by a geographically variable but vertically uniform horizontal shortening at a rate $\dot{\epsilon}$ equal to the seismic/brittle strain rate, $\dot{\epsilon}_H$. Incompressibility (or mass conservation at the scale of the lithosphere) implies that this horizontal shortening must be accompanied by a vertical thickening of the lithosphere at a rate $\dot{\epsilon}_V = -\dot{\epsilon}_H$, assuming that horizontal deformation in a direction perpendicular to the direction of maximum shortening is negligible.

If we assume, as proposed earlier, that the current state of compression felt by the Australian continent originated at the time of the collision across the South Island of New Zealand started (i.e. 10–8 Ma), we can estimate the total amount of thickening experienced by the various parts of the continent by integrating the computed vertical strain rate over 10 Ma:

$$\epsilon_V = \dot{\epsilon}_V \times 10\text{Ma} \quad (6)$$

The computed vertical strain can then be used to compute the local lithospheric thickening, and, by assuming local isostatic equilibrium, the amount of uplift, u , experienced by each $2^\circ \times 2^\circ$ continental cell over the last 10 Ma:

$$u = h_c \epsilon_V \left(1 - \frac{\rho_c}{\rho_m} \right) \quad (7)$$

where h_c is crustal thickness, and ρ_c and ρ_m are average crustal and mantle rock densities, respectively. We used the $2^\circ \times 2^\circ$ CRUST2 model (Bassin *et al.* 2000) to obtain these values. We call u the ‘seismic uplift,’ that is the amount of rock uplift predicted from the seismic energy release measured over the past 50 years and

extrapolated over the past 10 Ma. The computed distribution of u is shown in Figure 4c and d, where it is compared with the current topography (Figure 4a) and a smoothed version of the present-day topography (Figure 4b) obtained by simply finding the maximum elevation within each $2^\circ \times 2^\circ$ cell.

We also estimated the effect of the lateral strength of the continental lithosphere by calculating the surface deflection of a thin elastic plate of variable thickness to the load created by the computed crustal thickening. Assuming a uniform crustal thickness of 40 km, we transformed the estimates of vertical strain into a spatially variable flexural load using a multi-grid version of the finite difference method described in van Wees & Cloetingh (1994). Effective elastic plate thickness values were derived from the most recent estimates of Swain & Kirby (2006) and range between 10 and 115 km. Other elastic parameters used are 7×10^{10} Pa for Young’s modulus and 0.25 for Poisson’s ratio. The results are shown in Figure 5 and differ only slightly from those obtained under the assumption of local isostatic equilibrium. This is not surprising as the spatial resolution of our strain and thus load estimates ($2^\circ \times 2^\circ$ or ~ 200 km) is comparable with the flexural wavelength of the lithosphere.

RESULTS

The computed seismic strain rate field is characterised by three distinct features that appear consistently in all estimates (Figure 3a–c): the southeastern Highlands, the Flinders Ranges and the southern part of the Yilgarn Craton (including the Albany–Fraser area), labelled 1–3 in Figure 2a, respectively. Those regions are characterised by high seismic strain rate (10^{-16} to 10^{-15} /s) and these estimates appear to be quite robust features of the continent current deformation pattern as they persist when the strain rate map is produced at a $1^\circ \times 1^\circ$ resolution. In the east, regions 1 and 2 are also characterised by high present-day topography (2000 m maximum elevation in the southeastern Highlands and up to 1000 m in the Flinders Ranges) and significant local relief, whereas region 3 in the Archean Yilgarn Craton is relatively low (i.e. < 400 m high) (Figure 2), and has little relief except along the seismically inactive Darling escarpment (Figure 2). Parts of northwestern Australia Canning Basin appear to be deforming at large rates ($\approx 10^{-15}$ /s) but that deformation is more diffuse and disappears when estimated on a $1^\circ \times 1^\circ$ grid (Figure 3c). This is because many of these smaller cells do not contain at least 20 events. It could alternatively be linked to the incompleteness of the seismic record in these more remote parts of the continent.

Note that not removing the aftershocks does not greatly modified the main features of the strain rate distribution (Figure 3b), except for the region located around the recent Tennant Creek earthquake in northern central Australia.

Our calculations suggest that several regions are not currently deforming at a substantial rate despite a noticeable seismic activity: these include the coastal areas of Southeastern Queensland, and central Australia.

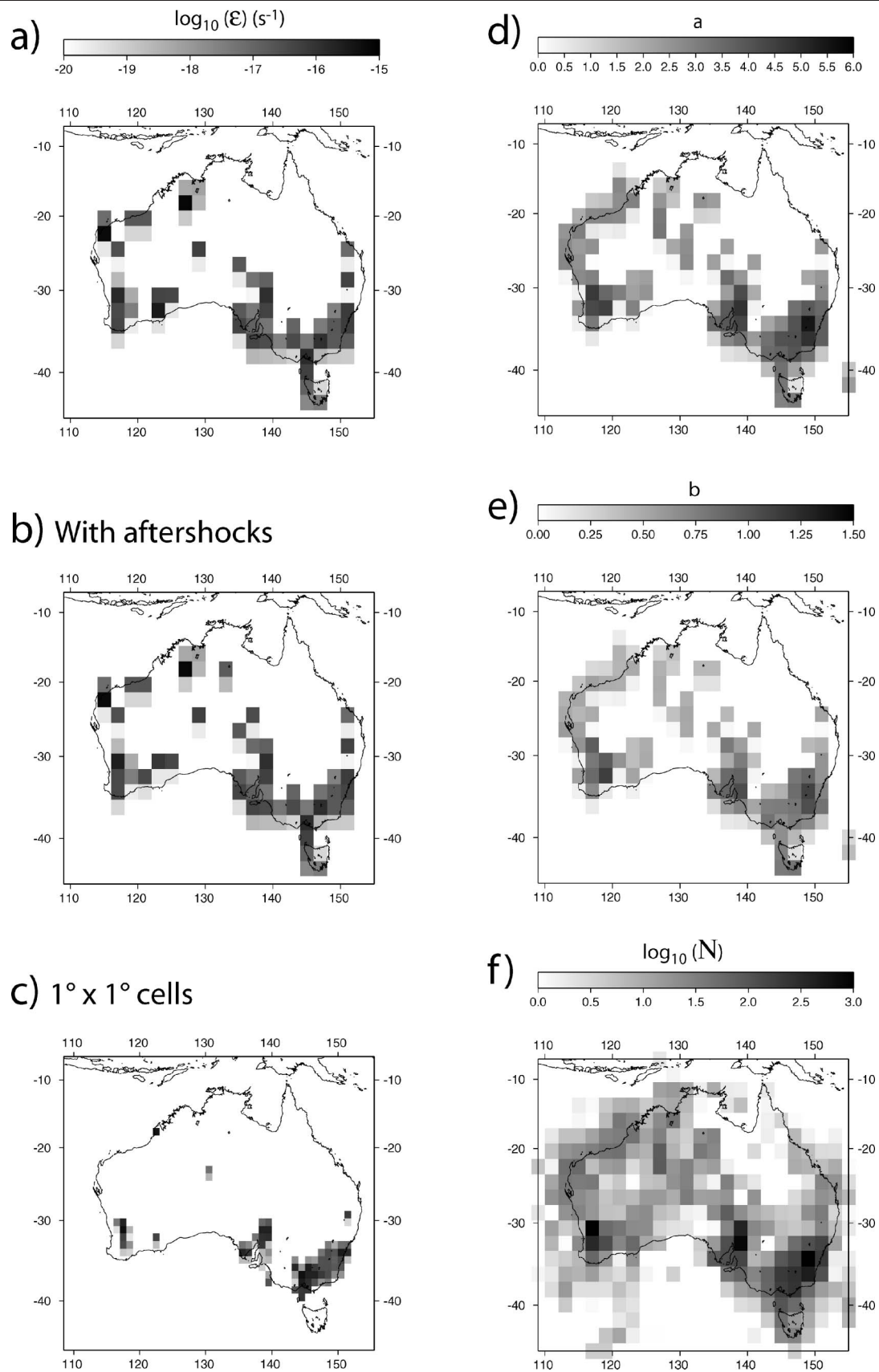
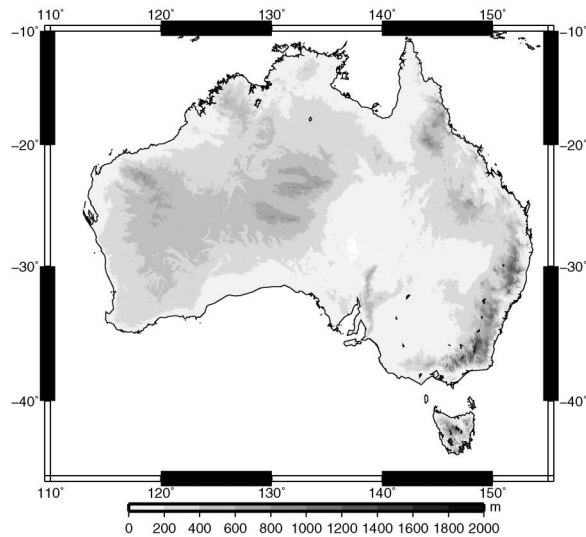
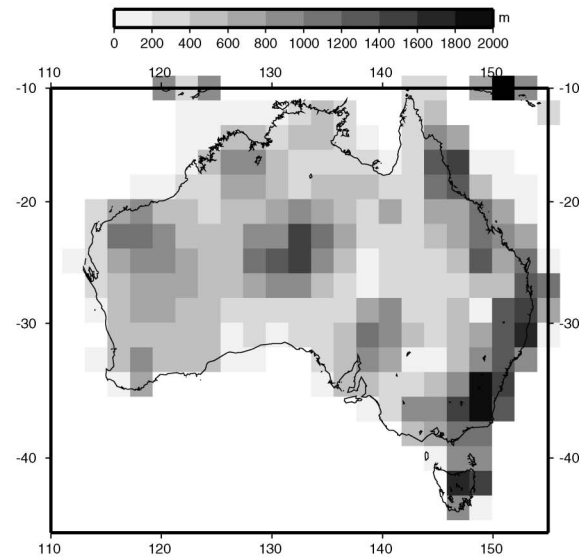


Figure 3 (a–c) Seismic strain rate as predicted from the distribution and magnitude of earthquakes observed over the 1970–2007 period assuming: (a) a maximum earthquake magnitude, M_{\max} of 7, aftershocks removed and a $2^\circ \times 2^\circ$ binning of the data; (b) without removing the aftershocks; and (c) a $1^\circ \times 1^\circ$ binning of the data. (d, e) Computed a and b values corresponding to (a). (f) Earthquake distribution, i.e. number of events in each cell.

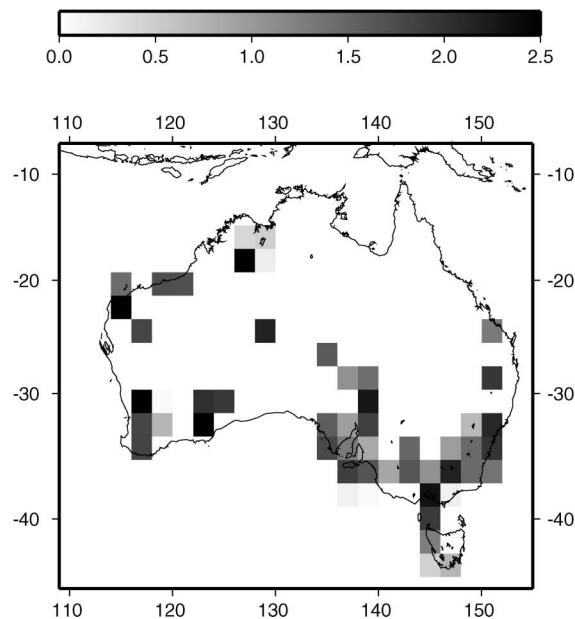
a) Present-day topography



b) Filtered topography



c) \log_{10} predicted topography



d) Predicted topography

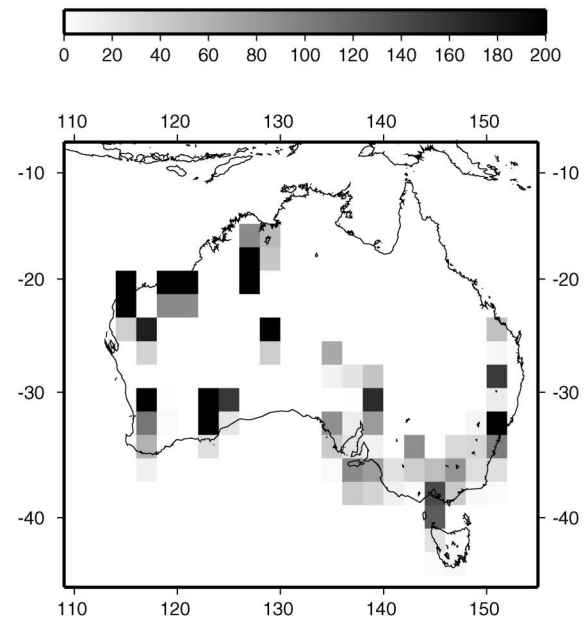


Figure 4 (a) Present-day topography. (b) Filtered topography, i.e. maximum topography in $2^\circ \times 2^\circ$ bins. (c, d) Predicted seismic uplift obtained by extrapolating current strain rate over a 10 Ma period and assuming (c) local isostasy and (d) flexural isostasy.

This simply reflects the low magnitude character of the historical seismic record in this regions. Furthermore, other regions are devoid of almost any seismic activity, including the Gawler Craton (Figure 2) in southern Australia and the northeastern part of the continent.

The computed a and b values are in an acceptable range ($0 < a < 6$ and $b \approx 1$) and similar to those obtained by Leonard (2008) using a less up to date seismic database.

In a number of regions there appears to be a good correlation between the predicted seismic uplift (Figure 4d) and the present-day topography (Figure 4b), suggesting that a substantial portion of the present-day topography has formed in recent time. Regions of high present-day topography where substantial seismic uplift is predicted includes the southeastern Highlands, the Flinders Ranges, central Australia, and the northeastern and southwestern boundaries of the Canning Basin.

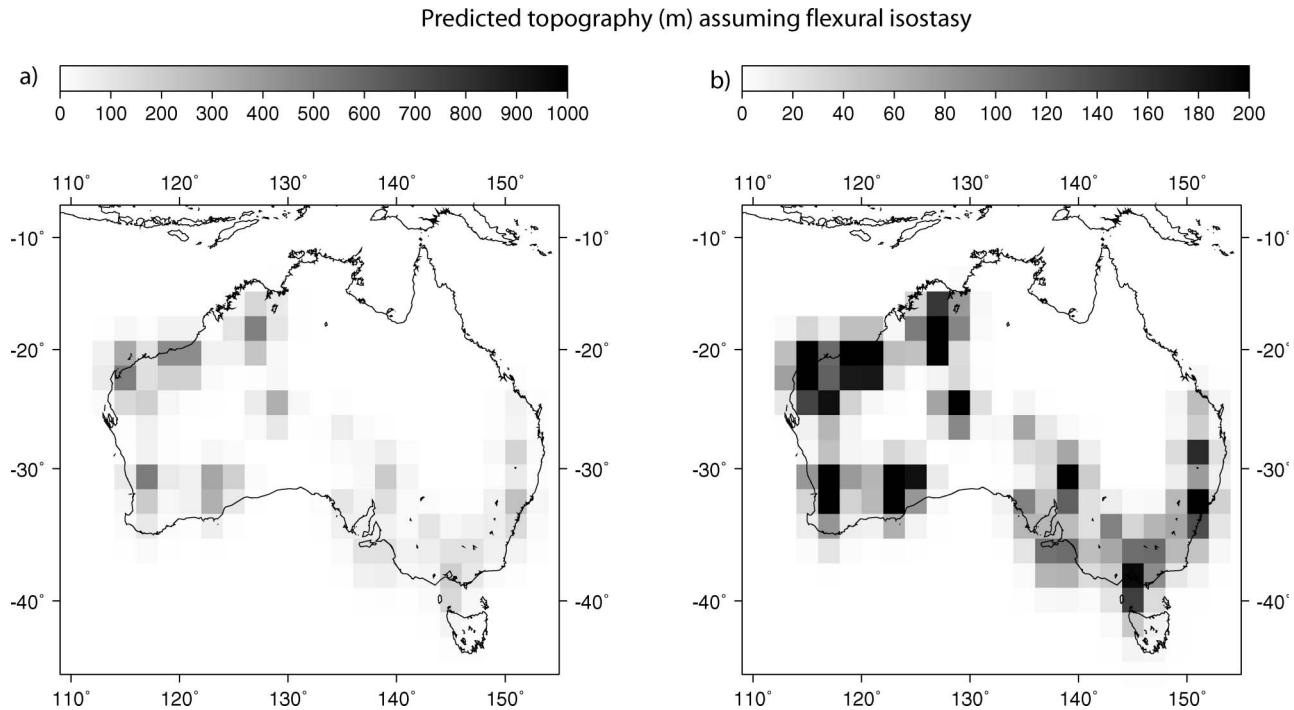


Figure 5 Predicted seismic uplift obtained under the assumption of regional, flexural isostasy. (a) and (b) represent the same results; they differ by the scale used to highlight different aspects (low and high amplitude) of the computed topography.

However, the high seismic activity and resulting seismic uplift along the southern part of the Yilgarn Craton and the Albany–Fraser region are not matched by noticeable present-day elevated topography and, conversely, the coastal areas of northern Queensland have substantial present-day topography but little predicted seismic uplift.

HOW TO EXPLAIN THE STRAIN LOCALISATION?

A continental wide seismic tomography survey (SKIPPY: van der Hilst *et al.* 1994, 1998) has provided evidence of a relatively complex seismic velocity structure within the lithosphere beneath the Australian continent (Figure 6). The eastern part of the continent is characterised by a relatively thin lithosphere, i.e. anomalously slow velocities at a depth of 100 km, whereas the regions to the west of the so-called Tasman Line, separating Proterozoic from Phanerozoic terrains are characterised by a deep lithospheric mantle root, i.e. anomalously high velocities at 100 km.

In the eastern part of the continent, seismic activity, and the associated strain and uplift are concentrated in belts of relatively thin, hence weak, lithosphere, locally associated with high surface heat flow, such as in the Flinders Ranges (McLaren *et al.* 2003). Deformation takes place in the southeastern Highlands, the Flinders Ranges and, to a lesser degree, in the coastal highlands of Queensland (labelled 1, 2 and 7, respectively, on Figure 2a) where, at the spatial resolution of the tomographic data (400 km), the SKIPPY data suggest that the lithosphere is thinner than in adjacent regions. Similarly, the basement beneath the Eromanga and

Murray Basins (labelled 8 and 9, respectively, on Figure 2a) appears ‘colder’ (Figure 6) and is characterised by reduced seismic activity and little or no deformation in the last 10 Ma (Figure 3). This suggests that in eastern Australia, it is the lithospheric strength (or rigidity) which determines which part of the continent is currently deforming.

In the west, this correlation between regions of active seismic deformation and the presence of relatively weak lithosphere breaks down. Apart from the westernmost tip of Western Australia, none of the currently deforming regions seem to be characterised by relatively low seismic velocities at 100 km depth, and those regions that are, do not deform. Thus, this suggests that the western part of the continent responds to the present-day compressive stress in a different manner from what is happening elsewhere. We hypothesise that, in the older (Precambrian) parts of the Australian continent, the lower, ductile part of the lithosphere is uniformly strong and deforms uniformly, whereas the upper (seismogenic) layer accommodates this large-scale flow by localised yet transient brittle deformation, potentially in zones of pre-existing crustal weakness. In short, lithospheric structures control deformation in the younger parts of the continent whereas crustal structures control deformation in the older, western regions, because the underlying lithospheric mantle is uniformly strong.

GEOMORPHIC RESPONSE TO SLOW SURFACE UPLIFT

Our computations have shown that several parts of the Australian continent are currently experiencing

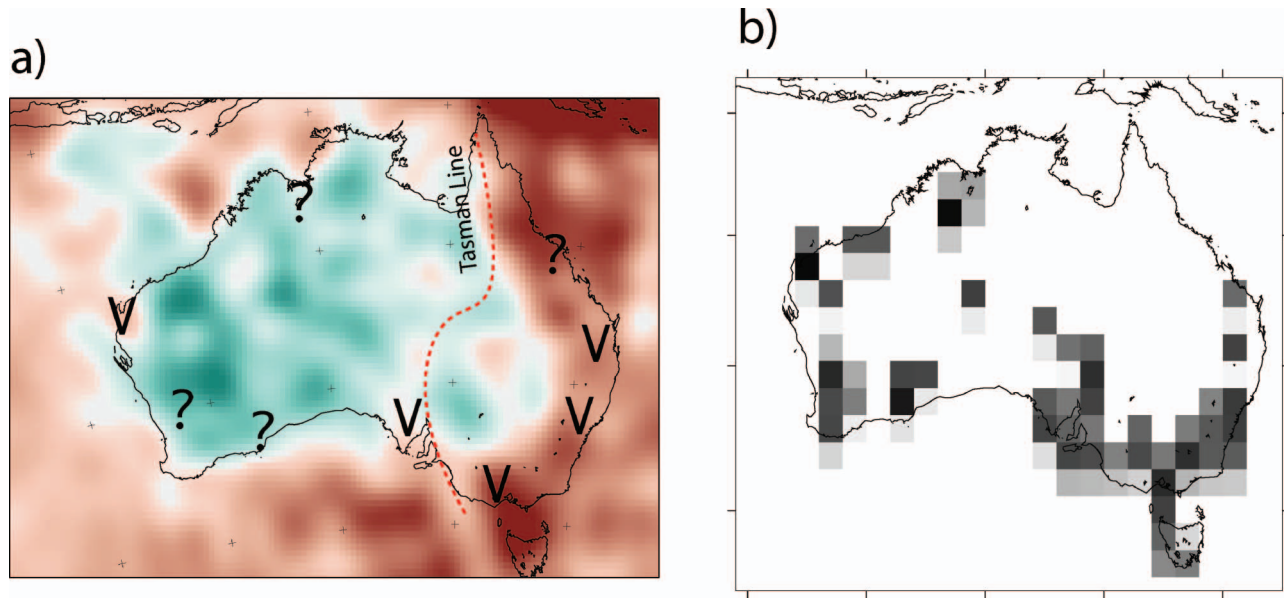


Figure 6 (a) Horizontal cross-section at 100 km depth through the deviation in seismic velocity from a mean reference velocity derived from the SKIPPY data. Darkest red areas correspond to a relative deviation of -8% ; darkest blue areas correspond to a relative deviation of 8% (Fishwick *et al.* 2005). (b) Computed seismic strain rate for comparison. Question marks indicate regions where there is no match between deformation and present-day topography; V-symbols indicate where this match is present.

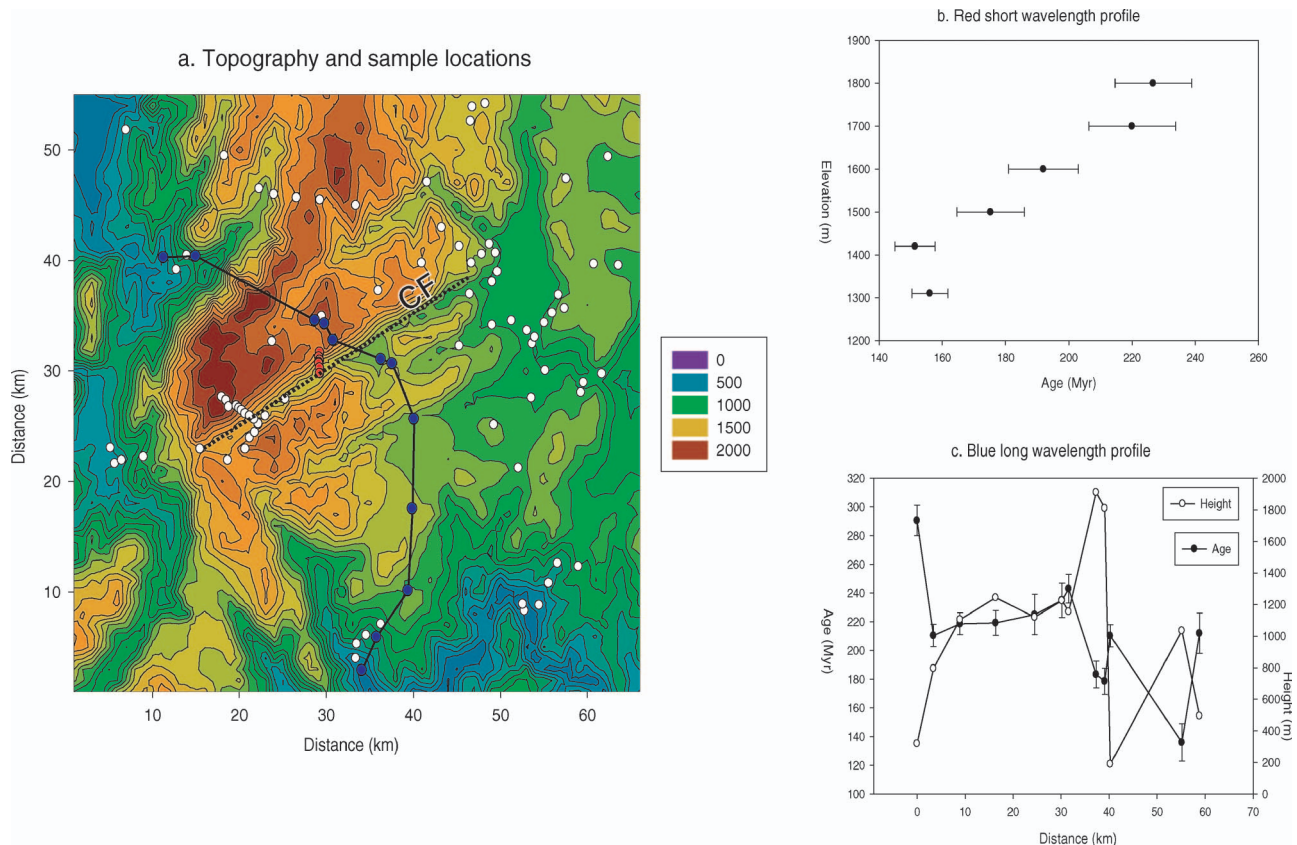


Figure 7 (a) Location of samples for fission-track apatite ages in the Snowy Mountain area of the southeastern Highlands (circles) superimposed on the topography. Location of red and blue profiles are also shown. Dotted line (CF) is trace of Crackenback Fault. (b) Age vs elevation along the red profile. (c) Age and elevation along the blue profile from southeast to northwest.

deformation and uplift. In the eastern part of the continent this has led to an apparent rejuvenation of the surface relief whereas in the west no significant surface relief has been formed recently. We propose two potential explanations for the apparent lack of correlation between topography and seismic/brittle deformation in the western part of the continent. The first one is that the current pattern of deformation, i.e. seismic strain is localised in the southwestern corner of the Yilgarn Craton and is not representative of the distribution of deformation over geological time-scales; in other words the current pattern is transient. This may result from the mechanical properties of the lithosphere underlying Western Australia. The area is known to be characterised by a low surface heat flux (Cull 1982) and a relatively thick lithospheric mantle (Simons *et al.* 1999; Debayle & Kennett 2000a, b; Simons & van der Hilst 2003), suggesting that it is characterised by a cold geotherm in comparison with other parts of the continent which, in turn, implies a relatively strong lithospheric mantle. Lateral strength variations are also likely to be less pronounced in such a cold environment. It is therefore possible that deformation of the western part of the Australian continent takes place by uniform shortening of the mantle lithosphere and that strain localisation takes place in the upper, brittle layer only along pre-existing tectonic, crustal boundaries. However, another consequence of the relatively cold geotherm characterising the area is that there is no decoupling between crustal and mantle deformation, implying that over geological time-scales, deformation of the upper crust must also be spatially uniform and little strain accumulation, and hence topography, develops.

An alternative scenario is based on the observation that, contrary to what has happened in the eastern part of the continent, there was no pre-existing elevated topography and/or surface relief in the southwest prior to 10 Ma. Therefore, the landforming processes are quite different on either side of the continent; where there is topography, geomorphological processes are dominated by those proportional to slope, such as fluvial erosion and hill-slope soil transport, whereas, where no substantial relief exists, the dominant processes may be eolian transport, flooding and/or rain splash. Furthermore, as most of the uplift is the result of shortening that is accommodated in the upper crust by brittle failure and thus faulting, it is possible that the dominant landforming mechanisms active in the relatively flat western part of the continent are more efficient at eroding away surface relief caused by near-surface faulting (such as the metre-high scarp created during the 1968 M 6.9 Meckering earthquake). This could explain why no substantial relief has formed in the western parts of the continent. We recognise that this hypothesis is very speculative, but it deserves further investigation.

HOW OLD IS THE TOPOGRAPHY?

It has been proposed that most of Australia's present-day topography is the eroded remnant of much taller mountain belts that formed in the Neoproterozoic and Paleozoic (Lambeck & Stephenson 1986). The Eastern

Highlands formed by accretion of continental fragments during the Lachlan, Tasman and Thomson orogenic events. The Flinders Ranges may represent what is left of a large mountain belt that formed during the Delamarian collision in the Neoproterozoic. Evidence also shows that most of the present-day topography is the result of movement on relatively old structures (mostly thrust faults) that developed during ancient orogenic events (Gray & Foster 1998). However, what is less clear is the age of the movement that has led to the formation of the present-day relief (Ollier & Pain 1994). Some of the present-day topography appears relatively young (younger than 10 Ma) and many of these regions geomorphologically active: the Adelaide Hills are characterised by steep topographic gradients, the Eastern Highlands are the locus of many landslides, and major network reorganisations (such as along the Snowy River) have taken place in the last few tens of millions of years (Fabel & Finlayson 1992).

It has been shown that by considering the relationship between elevation and the age of rocks determined by a low-temperature thermochronological system such as fission-track or (U-Th)/He dating in apatite, one can obtain information on the 'age' of a landform (Braun 2002). At short wavelength, the slope of an age-elevation transect provides information on the mean exhumation rate that is independent of the past geothermal gradient and/or the evolution of the surface relief. At long wavelength the relationship between age and elevation provides estimates of the rate of change in topographic relief amplitude since the rocks cooled through their closure temperature (i.e. the mean rock age), under the assumption that the position of the main features of the landform (the valleys) has not changed through time. A positive correlation between age and elevation implies that the amplitude of the relief has increased; a negative correlation implies a relative decrease in relief amplitude with time (Braun 2002).

An extensive apatite fission-track age database that covers many parts of the Australian continent has been assembled over the past 20 years (Kohn *et al.* 1999, 2002; Gleadow *et al.* 2002). In the Eastern Highlands, most of the ages are old, i.e. between 250 and 100 Ma. In Figure 7b and c, we show how age varies with elevation along a narrow near-vertical profile (red circles in Figure 7a) and a northwest-southeast profile (blue circles in Figure 7a), built from the fission-track database (Kohn *et al.* 2002). The long profile has been selected to cross regions of high-amplitude topographic relief in a direction approximately perpendicular to the strike of the relief. The results show an anti-correlation between age and elevation at long wavelength (≈ 100 km: Figure 7c) and a strong positive correlation at short wavelength (≈ 2.5 km: Figure 7b). From this we can estimate that the average denudation rate over the last 100–200 Ma has been slow (of the order of 1–5 m/Ma) and that over the same period of time, the relief has decreased by a factor of ~ 2 –3 using the spectral method described in Braun (2002). Alternatively, the large step in age with elevation along the long profile could be related to recent movement along the Crackenback Fault, shown on Figure 7a. Differential uplift (and thus exhumation) caused by fault movement could be the

dominant factor that perturbed the age distribution, in which case the spectral method proposed by Braun (2002) cannot be used, as it requires a uniform denudation rate over the sampled area. On the other hand, if fault movement is responsible for steps in age along the profile, this implies that the area has been deforming in the last 100–200 Ma and is therefore consistent with our interpretation of the seismic data that the region is actively deforming and that some of the topography/relief has been created recently.

However, there is no direct evidence in the thermochronological data of rejuvenation of the relief in the last 10 Ma. This implies that any relief that may have been created in the last 100 Ma did not cause sufficient incision and/or denudation to reset thermochronological ages, even for low-temperature systems such as apatite fission track. This puts a bound on the amount of topographic relief that may have been produced in the last 10 Ma (i.e. < 1 km) which is consistent with the uplift estimate based on integrating the seismic database (Figure 3).

CONCLUSIONS

We have demonstrated that the Australian continent is currently undergoing a slow but noticeable deformation. Based on a spatial and temporal integration of earthquake data, we have been able to provide meaningful bounds on the rate at which the continent is deforming today as well as a first-order picture of the spatial distribution of the deformation. Because the geometry and nature of the forces causing the deformation are relatively well known, the stress field that they generate within the continental block is relatively well constrained and fits the observations we have from borehole measurements and other stress indicators (Reynolds *et al.* 2002). Consequently, the Australian continent can be regarded as a natural laboratory where the relationship between strain and stress within continental interiors, i.e. the rheology of the continent, can be studied. Knowledge of the continent structure, thermal state and composition could also be used to constrain such a rheological model; this would include crustal thickness, thickness of sedimentary cover, surface heat flow, seismic velocity structure, etc. Work is under way to build such a rheological model.

ACKNOWLEDGEMENTS

This work was partly supported by an ARC Discovery Grant. We thank two anonymous journal reviewers for comments made on an earlier version of this manuscript.

REFERENCES

- BASSIN C., LASKE G. & MASTERS G. 2000. The current limits of resolution for surface wave tomography in North America. *EOS* **81**, F897.
- BATT G. E. & BRAUN J. 1999. The tectonic evolution of the Southern Alps, New Zealand: insights from fully thermally coupled dynamical modelling. *Geophysical Journal International* **136**, 403–420.
- BATT G. E., BRAUN J., KOHN B. P. & MCDUGALL I. 2000. Thermochronological analysis of the dynamics of the Southern Alps, New Zealand. *Geological Society of America Bulletin* **112**, 250–266.
- BRAUN J. 2002. Estimating exhumation rate and relief evolution by spectral analysis of age-elevation datasets. *Terra Nova* **14**, 210–214.
- BURBIDGE D. 2004. Thin-plate neotectonics models of the Australian plate. *Journal of Geophysical Research* **109**: B10405, doi:10.1029/2004JB003156.
- DE CARITAT P. & BRAUN J. 1992. Cyclic development of sedimentary basins at convergent plate margins. 1. Structural and tectono-thermal evolution of some Gondwana basins of eastern Australia. *Basin Research* **16**, 241–282.
- CLOETINGH S. & WORTEL R. 1986. Stress in the Indo-Australia plate. *Tectonophysics* **132**, 49–67.
- COBLENTZ D. D., SANDIFORD M., RICHARDSON R. M., ZHOU S. & HILLIS R. R. 1995. The origins of the intraplate stress field in continental Australia. *Earth and Planetary Science Letters* **133**, 299–309.
- COBLENTZ D. D., ZHOU S., HILLIS R. R., RICHARDSON R. M. & SANDIFORD M. 1998. Topography, boundary forces, and the Indo-Australian intraplate stress field. *Journal of Geophysical Research* **103**, 919–931.
- CULL J. P. 1982. An appraisal of Australian heat-flow data. *BMR Journal of Australian Geology & Geophysics* **7**, 11–21.
- DEBAYLE E. & KENNETT B. L. N. 2000a. Anisotropy in the Australian upper mantle from Love and Rayleigh wave inversion. *Earth and Planetary Science Letters* **184**, 339–351.
- DEBAYLE E. & KENNETT B. L. N. 2000b. The Australian continental upper mantle—structure and deformation inferred from surface waves. *Journal of Geophysical Research* **105**, 25423–25450.
- DENHAM D. 1988. Australian seismicity—the puzzle of the not-so-stable continent. *Seismological Research Letters* **59**, 235–240.
- DICKINSON J. A., WALLACE M. W., HOLDGATE G. R., GALLAGHER S. J. & THOMAS L. 2002. Origin and timing of the Miocene–Pliocene unconformity in southeast Australia. *Journal of Sedimentary Research* **72**, 288–303.
- DOYLE H. A. 1971. Seismicity and structure in Australia. *Bulletin of the Royal Society of New Zealand* **9**, 149–152.
- FABEL D. & FINLAYSON B. L. 1992. Constraining variability in south-east Australian long-term denudation rates using a combined geomorphological and thermochronological approach. *Zeitschrift für Geomorphologie NF* **36**, 293–305.
- FISHWICK S., KENNETT B. L. N. & READING A. M. 2005. Contrasts in lithospheric structure within the Australian craton—insights from surface wave tomography. *Earth and Planetary Science Letters* **231**, 163–176.
- GLEADOW A. J. W., KOHN B. P., BROWN R. W., O'SULLIVAN P. B. & RAZA A. 2002. Fission track thermotectonic imaging of the Australian continent. *Tectonophysics* **349**, 5–21.
- GRAY D. R. & FOSTER D. A. 1998. Character and kinematics of faults within the turbidite-dominated Lachlan Orogen: implications for tectonic evolution of eastern Australia. *Journal of Structural Geology* **20**, 1691–1720.
- GUTTENBERG B. & RICHTER C. F. 1944. Frequency of earthquakes in California. *Bulletin of the Seismological Society of America* **34**, 185–188.
- HILLIS R. R. & REYNOLDS S. D. 2000. The Australian stress map. *Journal of the Geological Society of London* **157**, 915–921.
- JACKSON J. A. 2002. Strength of the continental lithosphere: time to abandon the jelly sandwich? *GSA Today* **12**, 4–10.
- JOHNSTON A. C. 1994. Seismotectonic interpretations and conclusions from the stable continental region database. In: *The Earthquakes of Stable Continental Region Seismicity Database*, pp. 4–1–4–102. Electric Power Research Institute Report **TR-102261-1**.
- KOHN B. P., GLEADOW A. J. W., BROWN R. W., GALLAGHER K., O'SULLIVAN P. B. & FOSTER D. A. 2002. Shaping the Australian crust over the last 300 million years: insights from fission track thermotectonic imaging and denudation studies of key terranes. *Australian Journal of Earth Sciences* **49**, 697–717.
- KOHN B. P., GLEADOW A. J. W. & COX S. J. D. 1999. Denudation history of the Snowy Mountains: constraints from apatite fission track thermochronology. *Australian Journal of Earth Sciences* **46**, 181–198.
- KOSTROV V. V. 1974. Seismic moment and energy of earthquakes, and seismic flow of rocks. *Earth Physics* **1**, 23–40.
- LAMBECK K., MCQUEEN H. W., STEPHENSON R. & DENHAM D. 1989. The state of stress within the Australian continent. *Advances in Geophysics* **2**, 723–742.

- LAMBECK K. & STEPHENSON R. 1986. The post-Paleozoic uplift history of southeastern Australia. *Australian Journal of Earth Sciences* **33**, 253–270.
- LEONARD M. 2008. One hundred years of earthquake recording in Australia. *Bulletin of the Seismological Society of America* **98**, 1458–1470.
- MAGGI A., JACKSON J. A., MCKENZIE D. & PRIESTLEY K. 2000. Earthquake focal depths, effective elastic thickness, and the strength of the continental lithosphere. *Geology* **28**, 495–498.
- MCLAREN S., SANDIFORD M., HAND M., NEUMANN N., WYBORN L. & BASTRAKOVA I. 2003. The hot southern continent: heat flow and heat production in Australian Proterozoic terranes. In: Hillis R. R. & Müller R. D. eds. *Evolution and dynamics of the Australian Plate*, pp. 157–167. Geological Society of Australia Special Publication **22** and Geological Society of America Special Paper **372**.
- MOLNAR P. & TAPPONIER P. 1975. Cenozoic tectonics of Asia: effects of a continental collision. *Science* **189**, 419–426.
- OLLIER C. D. & PAIN C. P. 1994. Landscape evolution and tectonics in southeastern Australia. *AGSO Journal of Australian Geology & Geophysics* **14**, 335–345.
- PURCARU G. & BERCKHEMER H. 1978. A magnitude scale for very large earthquakes. *Tectonophysics* **49**, 189–198.
- QUIGLEY M., CUPPER M. & SANDIFORD M. 2006. Quaternary faults of southern Australia: palaeoseismicity, slip rates and origin. *Australian Journal of Earth Sciences* **53**, 285–301.
- REYNOLDS S. D., COBLENTZ D. D. & HILLIS R. R. 2002. Tectonic forces controlling the regional intraplate stress field in continental Australia: results from new finite element modeling. *Journal of Geophysical Research* **107**: 10.1029/2001JB000408.
- SANDIFORD M. 2003a. Geomorphic constraints on the late Neogene tectonics of the Otway Ranges. *Australian Journal of Earth Sciences* **50**, 69–80.
- SANDIFORD M. 2003b. Neotectonics of southeastern Australia: linking the Quaternary faulting record with seismicity and *in situ* stress. In: Hillis R. R. & Müller R. D. eds. *Evolution and Dynamics of the Australian Plate*, pp. 107–119. Geological Society of Australia Special Publication **22** and Geological Society of America Special Paper **372**.
- SANDIFORD M., WALLACE M. & COBLENTZ D. 2004. Origin of the *in situ* stress field in southeastern Australia. *Basin Research* **16**, 325–338.
- SCHOLZ C. H. 2004. *The Mechanics of Earthquakes and Faulting*. Cambridge University Press, Cambridge.
- SIMONS F. J. & VAN DER HILST R. D. 2003. Structure and deformation of the Australian lithosphere. *Earth and Planetary Science Letters* **211**, 271–286.
- SIMONS F. J., ZIELHUIS A. & VAN DER HILST R. D. 1999. The deep structure of the Australian continent from surface wave tomography. *Lithos* **48**, 17–43.
- SINADINOVSKI C. 2000. Computation of recurrence relation for Australian earthquakes: dams, fault scarps and earthquakes. *Australian Earthquake Engineering Society Conference Proceedings, Hobart*, pp. 22.1–22.5.
- SMITH R. I. 1990. Tertiary plate tectonic setting and evolution of Papua New Guinea. In: Carman G. J. & Carman Z. eds. *Petroleum Exploration in Papua New Guinea: Proceedings of the 1st PNG Petroleum Convention, Port Moresby*, pp. 261–290. Papua New Guinea Chamber of Mines, Port Moresby.
- SWAIN C. J. & KIRBY J. F. 2006. An effective elastic thickness map of Australia from wavelet transforms of gravity and topography using Forsyth's method. *Geophysical Research Letters* **33**: doi:10.1029/2005GL025090.
- TRIEP E. G. & SYKES L. R. 1997. Frequency of occurrence of moderate to great earthquakes in intracontinental regions: implications for changes in stress, earthquake prediction and hazard assessments. *Journal of Geophysical Research* **102**, 9923–9948.
- VAN DER HILST R. D., KENNETT B. L. N., CHRISTIE D. & GRANT J. 1994. Project SKIPPY explores the lithosphere and mantle beneath Australia. *EOS* **75**, 177, 180–181.
- VAN DER HILST R. D., KENNETT B. L. N. & SHIBUTANI T. 1998. Upper mantle structure beneath Australia from portable array deployments. In: Braun J., Dooley J., Goleby B., van der Hilst R. & Klootwijk C. eds. *The structure and evolution of the Australian lithosphere*, pp. 39–57. American Geophysical Union Geodynamics Series **26**.
- VAN WEES J. D. & CLOETINGH S. 1994. A finite difference technique to incorporate spatial variations in rigidity and planar faults into 3-D models for lithospheric flexure. *Geophysical Journal International* **117**, 179–195.
- VEEVERS J. J., JONES J. G. & POWELL C. McA. 1984. Synopsis. In: Veevers J. J. ed. *Phanerozoic Earth History of Australia*, pp. 351–364. Clarendon Press, Oxford.
- WATTS A. B. & BUROV E. B. 2003. Lithospheric strength and its relationship to the elastic and seismogenic layer thickness. *Earth and Planetary Science Letters* **213**, 113–133.
- WELLMAN H. W. 1979. An uplift map for the South Island of New Zealand, and a model for uplift of the Southern Alps. In: Walcott R. I. & Cresswell M. M. eds. *The Origin of the Southern Alps*, pp. 13–20. Bulletin of the Royal Society of New Zealand **18**.

Received 22 December 2007; accepted 5 July 2008